EMBO reports

scientific report

Detecting cAMP-induced Epac activation by fluorescence resonance energy transfer: Epac as a novel cAMP indicator

Bas Ponsioen[1,2], Jun Zhao[3*], Jurgen Riedl[3], Fried Zwartkruis[3], Gerard van der Krogt[1], Manuela Zaccolo[4], Wouter H. Moolenaar[2], Johannes L. Bos[3+] & Kees Jalink[1++]*

[1]Division of Cell Biology, and [2]Division of Cellular Biochemistry and Centre of Biomedical Genetics, The Netherlands Cancer Institute, Amsterdam, The Netherlands, [3]Department of Physiological Chemistry and Centre of Biomedical Genetics, UMCU, Utrecht, The Netherlands, and [4]Dulbecco Telethon Institute, Venetian Institute of Molecular Medicine, Padova, Italy

Epac1 is a guanine nucleotide exchange factor for Rap1 that is activated by direct binding of cAMP. *In vitro* studies suggest that cAMP relieves the interaction between the regulatory and catalytic domains of Epac. Here, we monitor Epac1 activation *in vivo* by using a CFP–Epac–YFP fusion construct. When expressed in mammalian cells, CFP–Epac–YFP shows significant fluorescence resonance energy transfer (FRET). FRET rapidly decreases in response to the cAMP-raising agents, whereas it fully recovers after addition of cAMP-lowering agonists. Thus, by undergoing a cAMP-induced conformational change, CFP–Epac–YFP serves as a highly sensitive cAMP indicator *in vivo*. When compared with a protein kinase A (PKA)-based sensor, Epac-based cAMP probes show an extended dynamic range and a better signal-to-noise ratio; furthermore, as a single polypeptide, CFP–Epac–YFP does not suffer from the technical problems encountered with multisubunit PKA-based sensors. These properties make Epac-based FRET probes the preferred indicators for monitoring cAMP levels *in vivo*.

Keywords: Epac; PKA; cAMP; FRET

EMBO reports (2004) **5**, 1176–1180. doi:10.1038/sj.embor.7400290

[1]Division of Cell Biology, and [2]Division of Cellular Biochemistry and Centre of Biomedical Genetics, The Netherlands Cancer Institute, Plesmanlaan 121, 1066CX Amsterdam, The Netherlands
[3]Department of Physiological Chemistry and Centre of Biomedical Genetics, UMCU, Universiteitsweg 100, 3584 CG Utrecht, The Netherlands
[4]Dulbecco Telethon Institute, Venetian Institute of Molecular Medicine, Via Orus 2, 35124, Padva, Padova, Italy
*These authors contributed equally to this work
[+]Corresponding author. Tel: +31 30 253 8988; Fax: +31 30 253 9035; E-mail: j.l.bos@med.uu.nl
[++]Corresponding author. Tel: +31 20 512 1933; Fax: +31 20 512 1944; E-mail: k.jalink@nki.nl

Received 30 June 2004; revised 4 October 2004; accepted 12 October 2004; published online 19 November 2004

INTRODUCTION

Cyclic AMP is a common second messenger that activates protein kinase A (PKA), cyclic nucleotide-regulated ion channels and Epac (for exchange proteins directly activated by cAMP). Epacs are guanine nucleotide exchange factors (GEFs) for Rap1 and Rap2 (de Rooij *et al*, 1998). Rap GTPases cycle between an inactive GDP-bound and an active GTP-bound state, with GEFs mediating the exchange of GDP for GTP. Rap proteins are involved in many biological processes, most notably the regulation of cell adhesion through integrins and cadherins (Bos, 2003). The GEF Epac1 consists of a C-terminal catalytic domain characteristic of exchange factors for Ras family GTPases and an N-terminal regulatory domain. The latter domain contains a cAMP-binding site similar to those of protein kinase A (PKA) and, in addition, a DEP domain that mediates membrane attachment (de Rooij *et al*, 1998; Rehmann *et al*, 2003a).

In vitro studies have shown that cAMP is absolutely required for the activation of Epac (de Rooij *et al*, 1998). It has been hypothesized that the regulatory domain of Epac functions as an auto-inhibitory domain, which is relieved from inhibition by cAMP, but direct proof for this notion is lacking. In this model, Epac is folded in an inactive conformation at low cAMP levels, thereby preventing Rap binding due to steric hindrance. cAMP binding unfolds the protein, allowing Rap to bind. This is somewhat analogous to the mechanism of PKA regulation by cAMP; in its inactive conformation, two regulatory subunits are bound to two catalytic subunits. On binding of cAMP, this complex falls apart, resulting in the release of active enzymes.

In the present study, we set out to measure Epac activation *in vivo* by sandwiching Epac between cyan fluorescent protein (CFP) and yellow fluorescent protein (YFP) and then measure fluorescence resonance energy transfer (FRET) between the two fluorescent moieties. FRET, the radiationless transfer of energy from a fluorescent donor to a suitable acceptor fluorophore, depends on fluorophore orientation and on donor–acceptor distance at a molecular scale. We show that in mammalian cells,

CFP–Epac–YFP displays significant energy transfer, which rapidly diminishes following a rise in intracellular cAMP and increases again in response to a fall in cAMP. This indicates that cAMP causes a significant conformational change *in vivo* and supports the unfolding model for Epac activation. Taking advantage of this property, we characterized CFP–Epac–YFP as a FRET sensor for cAMP and generated cytosolic, catalytically dead mutants. We show that the Epac-based cAMP indicators outperform the previously reported PKA-based cAMP sensor (Adams *et al*, 1991; Zaccolo *et al*, 2000; Zaccolo & Pozzan, 2002) in several aspects.

RESULTS AND DISCUSSION

cAMP induces a conformational change in Epac

To monitor cAMP-induced conformational changes in Epac, we generated a construct in which Epac1 was fused amino terminally to CFP and carboxy terminally to YFP, as shown in Fig 1A. Using a GST–RalGDS assay (supplementary information online), it was confirmed that this construct was able to activate Rap1. CFP–Epac–YFP was transiently expressed in human A431 cells, where it localized to membranes and the cytosol (see below). Fluorescence spectra of these cells revealed significant FRET (Fig 1B, red line), indicating that CFP and YFP are in close proximity (~3–4 nm). Stimulation with forskolin, a direct activator of adenylyl cyclase, significantly decreased FRET (green line). Similar responses were observed in other cell types, including HEK293, N1E-115 and MCF-7 cells. Thus, cAMP induces a significant conformational change in Epac, in support of the unfolding model (Fig 1A).

We next analysed the kinetics of cAMP-induced FRET changes by ratiometric recording of CFP and YFP emission using a dual-photometer set-up (see Methods). Within seconds after addition of forskolin, FRET started to decrease, usually dropping to a minimum level in 2–3 min (Fig 1C). In the presence of the phosphodiesterase inhibitor IBMX (100 μM), forskolin evoked an average decrease of 30±3% in CFP/YFP emission ratio. This reflects near-complete saturation of cAMP binding to Epac, as deduced from experiments where cells were subsequently permeabilized with digitonin (10 μg/ml) in the presence of 2 mM extracellular cAMP (Fig 1D). This caused at most a moderate (on average, ~3%) further drop in FRET.

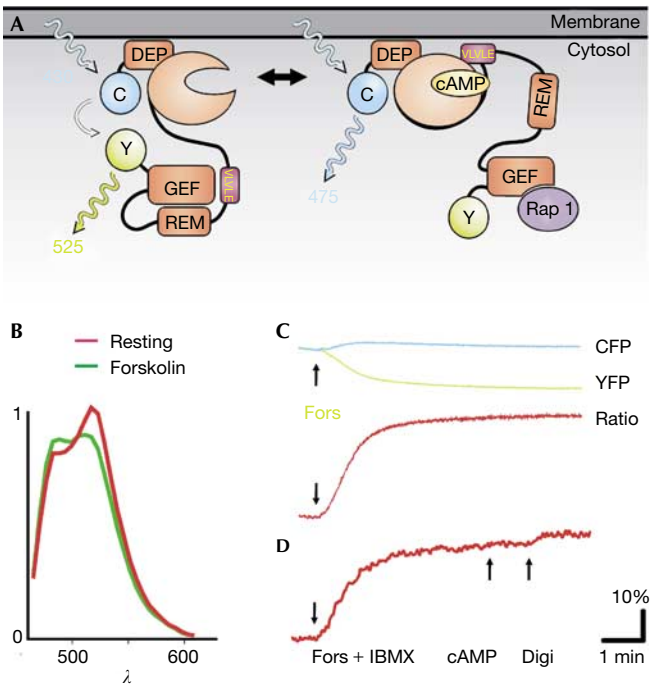

Fig 1 | cAMP-induced conformational change in Epac detected by FRET. (**A**) Model for the conformational change following binding of cAMP to the regulatory domain of Epac (adapted from Bos, 2003). Following cAMP binding, the VLVLE sequence can interact with the regulatory domain, releasing the inhibition of the GEF domain by the REM domain. FRET between the CFP and YFP tags allows detection of this conformational change. (**B**) Emission spectra of CFP–Epac–YFP, excited at 430 nm. Red line, resting level; green line, 3 min after forskolin treatment (25 μM). (**C**) Time course of cAMP-induced CFP–Epac–YFP activation, monitored in A431 cells by FRET. Increases in the ratio CFP/YFP reflect unfolding of Epac. The arrow indicates addition of forskolin (Fors, 25 μM). (**D**) Cells were treated with forskolin (25 μM) and IBMX (100 μM) and subsequently permeabilized using digitonin (Digi, 10 μg/ml) in the presence of 2 mM cAMP.

Epac activation is independent of subcellular localization

CFP–Epac–YFP localized to the cytosol and to membranes, in particular to the nuclear envelope and to perinuclear compartments. We confirmed proper targeting of CFP–Epac–YFP by comparing its distribution with that of immunolabelled endogenous Epac in OVCAR3 cells. Identical localization patterns were observed (Zhao *et al*, unpublished data), in agreement with a previous report (Qiao *et al*, 2002). Thus, CFP–Epac–YFP can be used as a FRET probe to image Epac activation. As activation of its downstream target Rap1 is membrane-delimited (Mochizuki *et al*, 2001; Bivona *et al*, 2004), we set out to visualize Epac activation throughout the cell by two different imaging FRET techniques (supplementary information online). The results show that, at least in these cells, agonists induce homogeneous FRET changes throughout the cell. Thus, Epac activation is not confined to membranes, indicating that cAMP binding is the main determinant of Epac activation.

CFP–Epac–YFP as a novel fluorescent cAMP indicator

Having shown that FRET changes in CFP–Epac–YFP reflect cAMP binding, we next investigated how well the Epac construct performs as an *in vivo* sensor for cAMP. We first tested whether CFP–Epac–YFP is insensitive to cGMP, given that cGMP binds to Epac with an affinity similar to that of cAMP, but fails to activate the enzyme (Rehmann *et al*, 2003b). In N1E-115 neuroblastoma cells, which express soluble guanylyl cyclase, a massive increase in intracellular cGMP levels ensued following stimulation with the NO donor sodium nitroprusside, as recorded by the cGMP-sensitive FRET sensor Cygnet-1 (Honda *et al*, 2001). In contrast, the Epac FRET signal was not affected by nitroprusside treatment (Fig 2A). We conclude that cGMP does not detectably affect the conformation of Epac.

We next tested two cAMP analogues that are specific for either Epac or PKA. As shown in Fig 2B, the Epac-specific compound 8-*p*-CPT-2′-*O*-Me-cAMP (Enserink *et al*, 2002) reduced FRET in the Epac-cAMP sensor but not in the PKA-cAMP sensor. Conversely, the PKA-specific compound 6-Bnz-cAMP (Christensen *et al*, 2003) specifically diminished the FRET signal only in cells expressing the PKA-based sensor (Fig 2B). Thus, the Epac-cAMP sensor preserves its specificity for cAMP analogues.

We further tested the Epac FRET construct in various cell types, including Rat-1 and NIH3T3 fibroblasts, mouse GE11 epithelial cells, mouse N1E-115 neuroblastoma and human MCF7 breast carcinoma cells. Addition of various cAMP-raising agents and receptor agonists, including forskolin, epinephrine, prostaglandin E1 and neurokinin A, caused robust FRET decreases in all cases. In general, forskolin induced a sustained decrease in FRET, whereas in most cell types, receptor agonists such as PGE1 and epinephrine (adrenaline) elicited transient signals lasting for 10–15 min (Fig 2C and data not shown). The transient nature of the epinephrine-induced signal is due to homologous receptor desensitization, as a second but distinct stimulus is still capable of decreasing FRET. We conclude that CFP–Epac–YFP is a specific, highly sensitive and reliable indicator of both transient and sustained changes in intracellular cAMP levels.

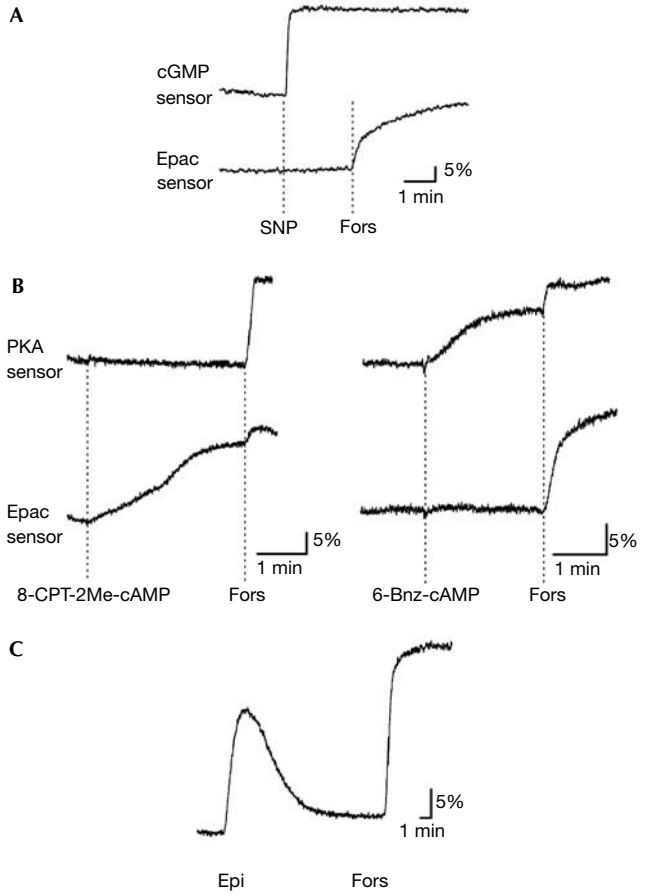

Fig 2 | CFP–Epac–YFP is a specific sensor for cAMP. (**A**) N1E-115 cells expressing either the cGMP sensor (Cygnet 2.1, upper trace) or the Epac-cAMP sensor (lower trace) were treated with sodium nitroprusside (SNP, 1 mM) and forskolin (25 μM). The traces depict cAMP- or cGMP-induced loss of FRET as an upward change in CFP/YFP ratio. (**B**) The PKA- and the Epac-cAMP sensor were tested for their sensitivity to 8-*p*-CPT-2′-*O*-Me-cAMP (8-CPT-2Me-cAMP, 100 μM), a specific activator of Epac, and 6-benzoyl-cAMP (6-Bnz-cAMP, 1 mM), which specifically activates PKA. In accordance with biochemical data (not shown), the slow and incomplete increases in CFP/YFP ratio in the upper right and lower left panels are caused by limited diffusion of these compounds over the plasma membrane. (**C**) Typical example of an agonist-induced cAMP response recorded with CFP–Epac–YFP in a Rat-1 fibroblast. Epi, epinephrine (250 nM); forskolin (25 μM) is added to calibrate the response.

Inactive, cytosolic mutants have increased FRET responses

To generate a cytosolic variant, we next deleted the DEP domain (amino acids 1–148), which is the main determinant of membrane localization (Qiao *et al*, 2002; Bos, 2003). Indeed, this chimaera, CFP–Epac(δDEP)–YFP, located almost exclusively in the cytosol (Fig 3A) in HEK293 and other cells. This mutation also diminished Epac's ability to activate Rap1 significantly (supplementary information online). We further introduced mutations (T781A, F782A) to render the indicator catalytically dead. These residues were predicted to affect Rap1 binding based on the crystal structure of SOS, a closely related GEF (Boriack-Sjodin *et al*, 1998). The resulting construct, CFP–Epac(δDEP-CD)–YFP, showed no detectable Rap1 activation (supplementary information online).

Spectral analysis revealed that the basal FRET level in the cytosolic variants was significantly above that of the full-length chimaera (Fig 3B). FRET in CFP–Epac(δDEP-CD)–YFP-expressing cells reliably decreased after stimulation with cAMP-raising agonists. Importantly, maximal changes in CFP/YFP ratio outperformed that of the full-length chimaera by about 50% in magnitude (~45 versus ~30%), significantly increasing the signal-to-noise ratio (Fig 3C). Because selectivity remained unaltered when compared with CFP–Epac–YFP (not shown), the cytosolic localization, catalytic inactivity and improved signal-to-

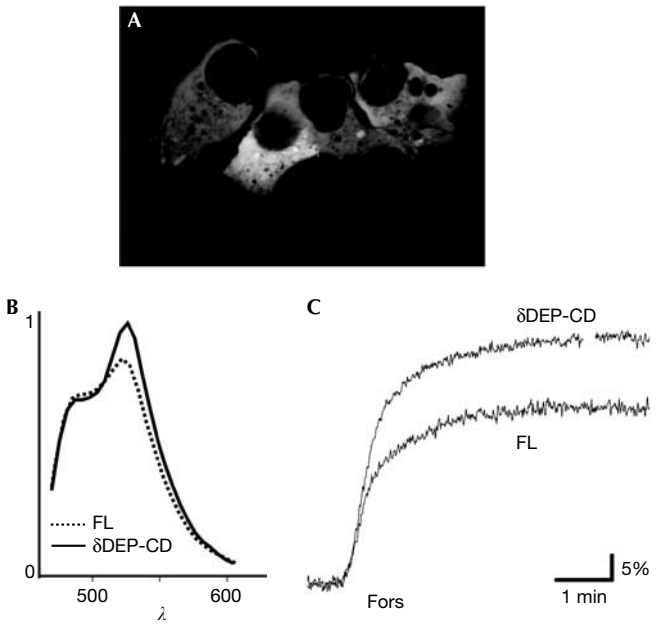

Figure 3 | CFP–Epac(δDEP-CD)–YFP is cytosolic, catalytically inactive and has improved signal-to-noise ratio. (**A**) Confocal micrograph of HEK293 cells expressing CFP–Epac(δDEP-CD)–YFP shows absence of membrane labelling. (**B**) Emission spectra of CFP–Epac–YFP (dashed line) and CFP–Epac(δDEP-CD)–YFP (solid line), excited at 430 nm. (**C**) Comparison of forskolin-induced change in CFP/YFP ratio in cells expressing CFP–Epac–YFP (FL) and CFP–Epac(δDEP-CD)–YFP. Representative traces from seven experiments each.

noise ratio make CFP–Epac(δDEP-CD)–YFP the indicator of choice for monitoring cytosolic cAMP levels.

Epac cAMP sensors display an extended dynamic range

Previously described PKA-based cAMP sensors are tetramers consisting of two catalytic and two regulatory domains. These probes contain four cAMP-binding sites and have submicromolar (~300 nM) affinity *in vivo* (Bacskai *et al*, 1993). cAMP binding in PKA shows cooperativity with an apparent Hill coefficient of 1.6 (Houge *et al*, 1990). As a consequence, this probe has a steep dose–response relationship that rapidly reaches saturation. In contrast, *in vitro* studies have shown that the affinity of the single cAMP-binding site in Epac is at least an order of magnitude lower (de Rooij *et al*, 2000). We determined the affinities of the different fluorescent Epac constructs for cAMP *in vitro* by fluorescence ratiometry (supplementary information online). The results showed affinities of ~50, ~35 and ~14 μM for CFP–Epac–YFP, CFP–Epac(δDEP)–YFP and CFP–Epac(δDEP-CD)–YFP, respectively. Thus, the Epac-cAMP sensors should display right-shifted and extended dynamic ranges.

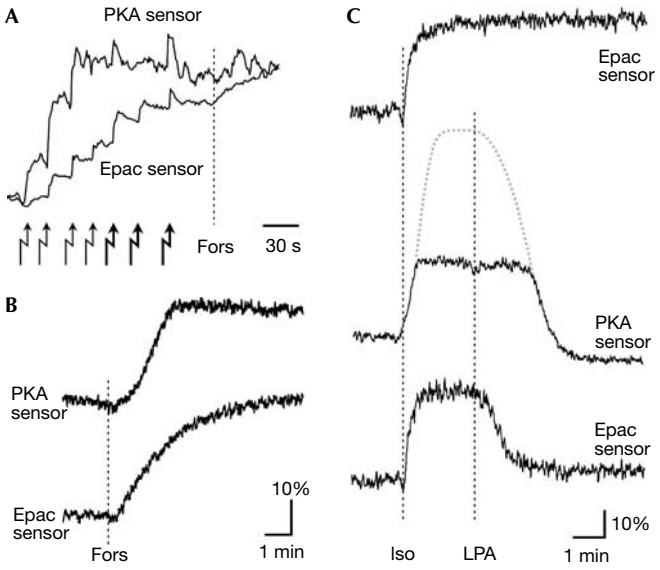

Figure 4 | The Epac-cAMP sensor exhibits an extended dynamic range as compared with the PKA-cAMP sensor. (**A**) Flash photolysis (thin arrows, 1/15 s; thick arrows, 1/4 s) of NPE-caged cAMP in neighbouring A431 cells expressing either PKA-cAMP or Epac-cAMP sensor (as recognized by partial decoration of membranes). Forskolin (50 μM) was added to further increase cAMP levels. Traces are normalized for comparison. (**B**) Typical responses to forskolin (50 μM), recorded with the PKA- and the Epac-cAMP sensor in A431 cells. Response rise times (10–90%) differed significantly (34 ± 5 s for PKA, $n = 9$; 248 ± 38 s for Epac, $n = 9$; $P < 0.005$). Note the sharp transition from the dynamic response range to the saturated plateau phase in the PKA sensor trace. (**C**) Upper trace: sustained cAMP elevation evoked by isoproterenol (isoprenaline; 10 μM) in a GE11 epithelial cell. Middle and lower traces: registration of cAMP decreases induced by subsequent addition of LPA (5 μM), visualized with the PKA probe and the Epac probe, respectively. Note that Epac reveals the immediate LPA effect, whereas it is obscured by saturation of the PKA-cAMP sensor.

To test this notion *in vivo*, cells expressing either CFP–Epac–YFP or the PKA-cAMP sensor were cocultured on coverslips, and neighbouring cells expressing comparable amounts of Epac and PKA, respectively, were analysed for FRET changes. Dosed photorelease of NPE-cAMP, a membrane-permeable caged cAMP analogue, was used to evoke identical incremental changes in intracellular cAMP in the two neighbouring cells (Fig 4A). Sequential increases in cAMP caused a rapid decrease in FRET and subsequent apparent saturation of the response in the PKA sensor, whereas the Epac sensor showed a much larger dynamic range. In line with these observations, the responses to forskolin-induced robust cAMP increases (Fig 4B) were rapid and saturating for the PKA-based sensor, whereas FRET in the Epac-based sensor changed more gradually and often did not saturate completely (Fig 1D).

The shifted and extended dynamic range of Epac for cAMP has important consequences for measuring physiological cAMP levels. As shown in Fig 4C, in GE11 cells, isoproterenol (isoprenaline) triggers a rapid and rather sustained FRET change (~30%). In isoproterenol-pretreated cells, addition of lysophosphatidic acid (LPA) resulted in a rapid recovery of the FRET signal, as one would expect for a Gi-coupled receptor agonist that lowers cAMP levels (van Corven *et al*, 1989). It is to be noted that the PKA-based sensor failed to record this rapid effect of LPA, apparently due to saturation of the probe, but rather reported a substantial lag period (up to several minutes; Fig 4C, middle trace). That it fails to record the true kinetics of the LPA-induced cAMP response becomes evident when the Epac-based sensor is used. As shown in Fig 4C, CFP–Epac–YFP detects the initial fall in cAMP levels within seconds after LPA addition.

CONCLUSIONS

Our results support a model in which cAMP binding to the regulatory domain of Epac releases an inhibitory conformation that prevents binding to Rap1 (de Rooij *et al*, 2000). Importantly, the FRET signal not only reflects binding of cAMP but also activation of Epac because cGMP, which binds with a similar affinity but fails to activate Epac (Rehmann *et al*, 2003b), is without effect. We used this property to show that the local, membrane-delimited activation of Rap1 (Mochizuki *et al*, 2001; Bivona *et al*, 2004) is not due to local activation of Epac. The uniform Epac activation here observed contrasts with the findings of Zaccolo & Pozzan (2002), who detected subcellular cAMP gradients in cardiac myocytes with the PKA-based cAMP sensor. This is probably explained by cell-type-specific differences in activity and intracellular distribution of the phosphodiesterases that shape such cAMP gradients, because we failed to detect gradients of cAMP using the PKA probe in our cells.

It is to be noted that our *in vivo* data on the basis of photolysis of NPE-caged cAMP (Fig 4A) strongly support the notion that cAMP differentially regulates its effectors, that is, low cAMP concentrations signal mainly through PKA, whereas at higher doses cAMP exerts additional effects through Epac activation (Zwartkruis *et al*, 1998).

This study further shows that Epac-based FRET constructs are ideally suited as cAMP sensors in that they exhibit improved characteristics compared with the commonly used PKA-based sensors. First, the moderate affinities of our Epac constructs (14–50 μM) result in a right-shifted dose–response relationship that matches physiological cAMP levels (Fig 4). During the review of this manuscript, a K_d of 2.3 μM was reported for a FRET sensor

based on Epac's isolated cAMP-binding domain (Nikolaev *et al*, 2004). Thus, Epac-based sensors provide a wide range of affinities that allows matching the sensors to the anticipated cAMP levels. Second, the PKA regulatory subunits each contain two cAMP-binding sites that exhibit cooperative binding (Hill coefficient of 1.6), resulting in a very steep response. In contrast, the single cAMP-binding domain of Epac1 results in an extended dynamic range. Third, Epac needs only a single cAMP molecule for a 30% FRET change, while four molecules of cAMP are needed to cause a comparable change in two donor–acceptor pairs in PKA. Together with the lower affinity of Epac, this results in reduced buffering of cytosolic cAMP. This is not trivial, as expression levels of cytosolic FRET probes commonly are in the micromolar range (0.1–5 μM; van der Wal *et al*, 2001), that is, at cAMP levels found in the cytosol following receptor stimulation. Fourth, the Epac-cAMP sensor is a single polypeptide, eliminating expression- and stoichiometry-related problems encountered with the PKA-based versions. For instance, unbalanced expression levels of regulatory and catalytic subunits of PKA hamper quantitative analyses of FRET changes. Furthermore, a single cDNA construct allows easy generation of stably transfected cell lines, which is often a problem with the PKA-based sensor (unpublished observations). Fifth, monomeric Epac sensors show faster activation kinetics than the slowly dissociating PKA-based sensors (Nikolaev *et al*, 2004). In addition, the cytosolic CFP–Epac(δDEP-CD)–YFP construct exhibits even larger cAMP-induced FRET changes, resulting in a superior signal-to-noise ratio. Together, these properties make Epac-based FRET probes the preferred fluorescent indicators for monitoring elevated cAMP levels in living cells.

METHODS

Cell culture, transfections and live cell experiments. Cells were seeded on glass coverslips, cultured and transfected with constructs as described (van Rheenen *et al*, 2004). Experiments were performed in a culture chamber mounted on an inverted microscope in bicarbonate-buffered saline (containing (in mM) 140 NaCl, 5 KCl, 1 $MgCl_2$, 1 $CaCl_2$, 10 glucose, 23 $NaHCO_3$, with 10 mM HEPES added), pH 7.2, kept under 5% CO_2, at 37 °C. Agonists and inhibitors were added from concentrated stocks. Expression levels of fluorescent probes were estimated as described (van der Wal *et al*, 2001).

Dynamic FRET monitoring. Cells on coverslips were placed on an inverted NIKON microscope and excited at 425 nm. Emission of CFP and YFP was detected simultaneously through 470±20 and 530±25 nm band-pass filters. Data were digitized and FRET was expressed as ratio of CFP to YFP signals, the value of which was set to 1.0 at the onset of the experiments. Changes are expressed as per cent deviation from this initial value of 1.0.

Loading and flash photolysis of NPE-caged cAMP. Cells were loaded by incubation with 100 μM NPE-caged cAMP for 15 min. Uncaging was with brief pulses of UV light (340–410 nm) from a 100 W HBO lamp using a shutter. For comparison, traces were normalized with respect to baseline and final FRET values.

Supplementary information is available at *EMBO reports* online (http://www.emboreports.org).

ACKNOWLEDGEMENTS

We thank M. Platje for experimental help, M. Langeslag for artwork and Dr W. Dostmann for the Cygnet construct. This work was supported by the Dutch Cancer Society (to J.L.B. and W.H.M.), the Netherlands Organization for Scientific Research (Y.Z.), Telethon Italy (TCP00089), the European Union (QLK3-CT-2002-02149) and the Fondazione Compagnia di San Paolo (M.Z.).

REFERENCES

Adams SR, Harootunian AT, Buechler YJ, Taylor SS, Tsien RY (1991) Fluorescence ratio imaging of cyclic AMP in single cells. *Nature* **349:** 694–697

Bacskai BJ, Hochner B, Mahaut-Smith M, Adams SR, Kaang BK, Kandel ER, Tsien RY (1993) Spatially resolved dynamics of cAMP and protein kinase A subunits in *Aplysia* sensory neurons. *Science* **260:** 222–226

Bivona TG, Wiener HH, Ahearn IM, Silletti J, Chiu VK, Philips MR (2004) Rap1 up-regulation and activation on plasma membrane regulates T cell adhesion. *J Cell Biol* **164:** 461–470

Boriack-Sjodin PA, Margarit SM, Bar-Sagi D, Kuriyan J (1998) The structural basis of the activation of Ras by Sos. *Nature* **394:** 337–343

Bos JL (2003) Epac: a new cAMP target and new avenues in cAMP research. *Nat Rev Mol Cell Biol* **4:** 733–738

Christensen AE *et al* (2003) cAMP analog mapping of Epac1 and cAMP kinase. Discriminating analogs demonstrate that Epac and cAMP kinase act synergistically to promote PC-12 cell neurite extension. *J Biol Chem* **278:** 35394–35402

de Rooij J, Zwartkruis FJ, Verheijen MH, Cool RH, Nijman SM, Wittinghofer A, Bos JL (1998) Epac is a Rap1 guanine-nucleotide-exchange factor directly activated by cyclic AMP. *Nature* **396:** 474–477

de Rooij J, Rehmann H, van Triest M, Cool RH, Wittinghofer A, Bos JL (2000) Mechanism of regulation of the Epac family of cAMP-dependent RapGEFs. *J Biol Chem* **275:** 20829–20836

Enserink JM, Christensen AE, de Rooij J, van Triest M, Schwede F, Genieser HG, Doskeland SO, Blank JL, Bos JL (2002) A novel Epac-specific cAMP analogue demonstrates independent regulation of Rap1 and ERK. *Nat Cell Biol* **4:** 901–906

Honda A, Adams SR, Sawyer CL, Lev-Ram V, Tsien RY, Dostmann WR (2001) Spatiotemporal dynamics of guanosine 3′,5′-cyclic monophosphate revealed by a genetically encoded, fluorescent indicator. *Proc Natl Acad Sci USA* **98:** 2437–2442

Houge G, Steinberg RA, Ogreid D, Doskeland SO (1990) The rate of recombination of the subunits (RI and C) of cAMP-dependent protein kinase depends on whether one or two cAMP molecules are bound per RI monomer. *J Biol Chem* **265:** 19507–19516

Mochizuki N, Yamashita S, Kurokawa K, Ohba Y, Nagai T, Miyawaki A, Matsuda M (2001) Spatio-temporal images of growth-factor-induced activation of Ras and Rap1. *Nature* **411:** 1065–1068

Nikolaev VO, Bunemann M, Hein L, Hannawacker A, Lohse MJ (2004) Novel single chain cAMP sensors for receptor-induced signal propagation. *J Biol Chem* **279:** 37215–37218

Qiao J, Mei FC, Popov VL, Vergara LA, Cheng X (2002) Cell cycle-dependent subcellular localization of exchange factor directly activated by cAMP. *J Biol Chem* **277:** 26581–26586

Rehmann H, Prakash B, Wolf E, Rueppel A, de Rooij J, Bos JL, Wittinghofer A (2003a) Structure and regulation of the cAMP-binding domains of Epac2. *Nat Struct Biol* **10:** 26–32

Rehmann H, Schwede F, Doskeland SO, Wittinghofer A, Bos JL (2003b) Ligand-mediated activation of the cAMP-responsive guanine nucleotide exchange factor Epac. *J Biol Chem* **278:** 38548–38556

van Corven EJ, Groenink A, Jalink K, Eichholtz T, Moolenaar WH (1989) Lysophosphatidate-induced cell proliferation: identification and dissection of signaling pathways mediated by G proteins. *Cell* **59:** 45–54

van der Wal J, Habets R, Varnai P, Balla T, Jalink K (2001) Monitoring agonist-induced phospholipase C activation in live cells by fluorescence resonance energy transfer. *J Biol Chem* **276:** 15337–15344

van Rheenen J, Langeslag M, Jalink K (2004) Correcting confocal acquisition to optimize imaging of fluorescence resonance energy transfer by sensitized emission. *Biophys J* **86:** 2517–2529

Zaccolo M, Pozzan T (2002) Discrete microdomains with high concentration of cAMP in stimulated rat neonatal cardiac myocytes. *Science* **295:** 1711–1715

Zaccolo M, De Giorgi F, Cho CY, Feng L, Knapp T, Negulescu PA, Taylor SS, Tsien RY, Pozzan T (2000) A genetically encoded, fluorescent indicator for cyclic AMP in living cells. *Nat Cell Biol* **2:** 25–29

Zwartkruis FJ, Wolthuis RM, Nabben NM, Franke B, Bos JL (1998) Extracellular signal-regulated activation of Rap1 fails to interfere in Ras effector signalling. *EMBO J* **17:** 5905–5912